International Journal of Fracture **100:** 227–248, 1999.

A reappraisal of transition elements in linear elastic fracture mechanics

ARASH YAVARI[1], E. THOMAS MOYER JR.[2] and SHAHRAM SARKANI[3]
[1]*Graduate Research Assistant, School of Engineering and Applied Science, The George Washington University, Washington, D.C. 20052, U.S.A.*
[2]*Corporate Scientist, The Engineering Technology Center, Century Building, Suite 1250, 2341 Jefferson Davis Highway, Arlington, Virginia 22202, U.S.A.*
[3]*Professor, School of Engineering and Applied Science, The George Washington University, Washington, D.C. 20052, U.S.A.*

Received 24 February 1999; accepted in revised form 22 March 1999

Abstract. This article offers a detailed comparison of the transition elements described by P.P. Lynn and A.R. Ingraffea [*International Journal for Numerical Methods in Engineering* **12**, 1031–1036] and C. Manu [*Engineering Fracture Mechanics* **24**, 509–512]. The source of a numerical phenomenon in using Manu's transition element (TE) is explained. The effect of eight-noded TEs with different quarter-point elements (QPE) on the calculated stress intensity factors (SIFs) is investigated. Strain at the crack tip is shown to be singular for any ray emanating from the crack tip within an eight-noded TE, but strain has both $r^{-1/2}$ and r^{-1} singularities, with $r^{-1/2}$ dominating for large TEs. Semi-transition elements (STEs) are defined and shown to have a marginal effect on the calculated SIFs. Nine-noded transition elements are formulated whose strain singularity is shown to be the same as that of eight-noded TEs. Then the effect of eight-noded and nine-noded TEs with collapsed triangular QPEs, and rectangular and nonrectangular quadrilateral eight-noded and nine-noded QPEs, is studied, and nine-noded TEs are shown to behave exactly like eight-noded TEs with rectangular eight-noded and nine-noded QPEs and to behave almost the same with other QPEs. The layered transition elements proposed by V. Murti and S.Valliapan [*Engineering Fracture Mechanics* **25**, 237–258] are formulated correctly. The effect of layered transition elements is shown by two numerical examples.

Key words: Transition element, crack tip, fracture mechanics, finite elements.

1. Introduction

The calculation of the stress intensity factor (SIF) by the finite element method has attracted many researchers in the last two decades. For purposes of analyzing a cracked body, quarter-point crack tip elements have been the most successful. Quadratic quarter-point elements (QPE) were proposed independently by Henshell and Shaw (1975) and by Barsoum (1976, 1977). These singular elements have been used successfully to date in linear elastic fracture mechanics. Less successful have been efforts to characterize and utilize transition elements (TEs) to calculate SIFs. This study returns to the works that originated the concept of TEs to discover why the concept has not succeeded to date.

Lynn and Ingraffea (1978) introduced the concept of transition elements. They showed that, for the second layer of elements around the crack tip, by varying the placement of the mid-nodes between quarter-point and mid-point, the singularity point can be put at the crack tip. Lynn and Ingraffea calculated the position of the mid-node in terms of the lengths of the QPE and the TE. Then they used a layer of these transition elements adjacent to singular

elements and observed that, for small L_Q/a (the ratio of singular crack tip element length to crack length), using TEs improves the accuracy of the calculated stress intensity factors (SIFs). Yet Lynn and Ingraffea did not point out that, in their numerical example, reducing crack tip element length automatically increases L_T/L_Q (the ratio of TE length to QPE length). As a matter of fact, along with L_Q/a, L_T/L_Q also plays an important role in the effects of TEs on the accuracy of calculated SIFs.

Manu (1986) reconsidered this problem and obtained a different TE than had Lynn and Ingraffea. He showed that L_T/L_Q affects the effect of the TEs. Manu observed that using his TEs, for large L_T/L_Q ratios, the sign of the error in the SIFs changes. In this paper we explain this numerical phenomenon. Hussain, et al. (1981), extended the concept of transition elements to cubic isoparametric elements. They concluded that TEs improve the accuracy of results only when L_T/L_Q is large. They mentioned that the application of TEs has not been as successful as that of QPEs because, for these elements, 'the crack tip senses not only the square root singularity but also a stronger singularity' (p. 1404). Here, we will show this analytically. But this does not reveal the reason for the lack of success in previous applications of TEs: the problem with TEs is that they are effective only for large L_T/L_Q. Appendix 1 shows that the quadratic TE proposed by Hussain, et al. is the same as that found by Lynn and Ingraffea.

Other researchers have examined various aspects of TEs. Murti and Valliapan (1986) argued that transition elements were incorrectly formulated by Lynn and Ingraffea. They proposed that the transition element size must be at a certain ratio to that of the QPE. In their numerical analyses, they used layered transition elements and found them useful for calculating SIFs in deep cracks. Lim, et al. (1991), demonstrated that Manu, and Murti and Valliapan, incorrectly formulated their transition elements and that the original formulation by Lynn and Ingraffea is correct. Horva'th (1994) considered an nth order isoparametric element as a transition element for an $r^{(1-m)/m}$ strain singularity problem. She showed that in the special case of $m = n = 2$ her TEs are identical to the TEs found by Lynn and Ingraffea.

This paper offers a detailed comparison between Lynn and Ingraffea's and Manu's TEs and an explanation of underestimation of SIFs using Manu's TEs in Section 2. Strain singularity for an eight-noded TE along an arbitrary ray emanating from the crack tip is investigated in Section 3. In Section 4, nine-noded TEs are formulated and their strain singularity investigated. Semi-transition elements are introduced in Section 5. A correct formulation of the layered transition elements of Murti and Valliapan is presented in Section 6. Section 7 presents numerical results.

2. Transition elements according to Lynn and Ingraffea, and Manu

This section offers a detailed comparison of Lynn and Ingraffea's and Manu's TEs. Here, the mid-node position is called the 'transition point.' There has been controversy over the exact position of transition points of quadratic TEs.

Using Manu's notations (1986, Figure 1), for the quarter-point and transition element assemblage, Lynn and Ingraffea proposed the following relation between p and q

$$p = \frac{1 - q + \sqrt{q^2 + 2q}}{2}. \tag{1}$$

Manu proposed a different relation

$$p = \frac{2q + 1}{2(q + 1)}. \tag{2}$$

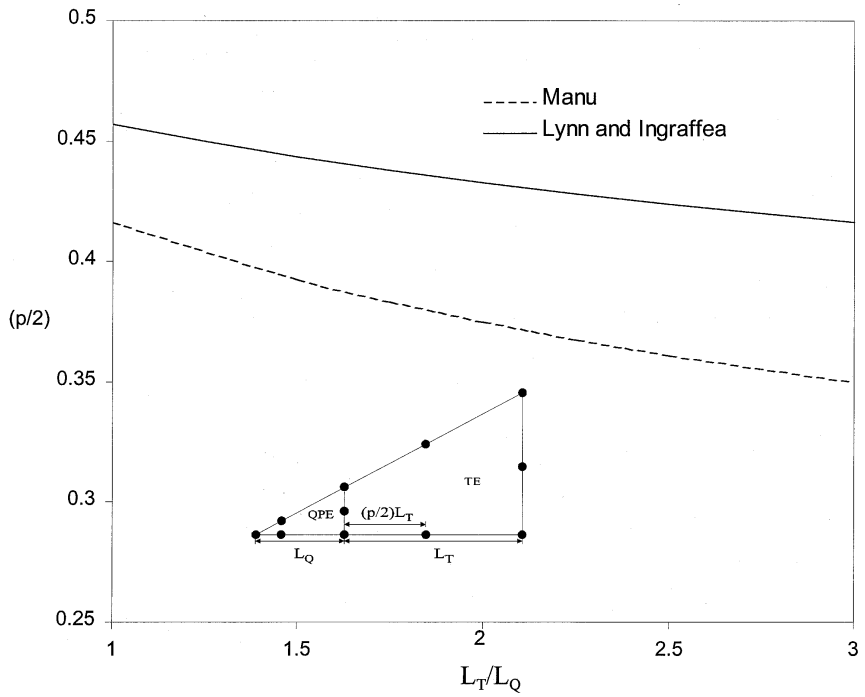

Figure 1. Manu's and Lynn and Ingraffea's transition points.

The variation of the position of the transition point $(p/2)$ versus the L_T/L_Q ratio is shown in Figure 1. For a standard element, $p/2 = 0.5$, and for a QPE, $p/2 = 0.25$. As can be seen, Manu's transition point is always closer to the crack tip than Lynn and Ingraffea's. The singularity point of Lynn and Ingraffea's TE is at the crack tip. When an incorrect value is used for a transition point, the singularity point will no longer coincide with the crack tip. For any L_T/L_Q, (2) gives a 'p.' Substituting this 'p' in (1), we obtain a 'q.' This 'q' value is not equal to $2L_Q/L_T$; it is equal to $2L'_Q/L_T$. If we assume a constant L_T, this means that we have a fictitious QPE whose length is L'_Q. The corner node of this fictitious QPE does not coincide with the crack tip. The distance between the crack tip and the corner node of this fictitious QPE is denoted by e (the eccentricity of the singularity point from the crack tip). In Figure 2 the variation of e/L_Q is shown. As can be seen, for very large L_T/L_Q values, the e/L_Q approaches unity. In Figure 3, Murti and Valliapan's TE (for $L_T/L_Q = \gamma_1 = 1.5524077$) is compared with the TE proposed by Lynn and Ingraffea and by Manu. It can be easily shown that for $L_T/L_Q = \gamma_1$

$$|e_{\text{Murti \& Valliapan}}| < |e_{\text{Manu}}|. \tag{3}$$

Manu observed that by using his transition element the sign of the error of the calculated K_{I} changes for large L_T/L_Q values. Later Lim et al. (1991), observed that for large L_T/L_Q ratios Manu's formulation yields substantially different results than those of Lynn and Ingraffea. They concluded that this 'large discrepancy can perhaps be expected because of the incorrect ε-q relationship' (p. 981) postulated by Manu. Now we present an explanation for this numerical phenomenon: In Lynn and Ingraffea's TE, the singularity point always coincides with the crack-tip independent of L_T/L_Q. In Manu's TE (Figure 4), as L_T/L_Q increases, the

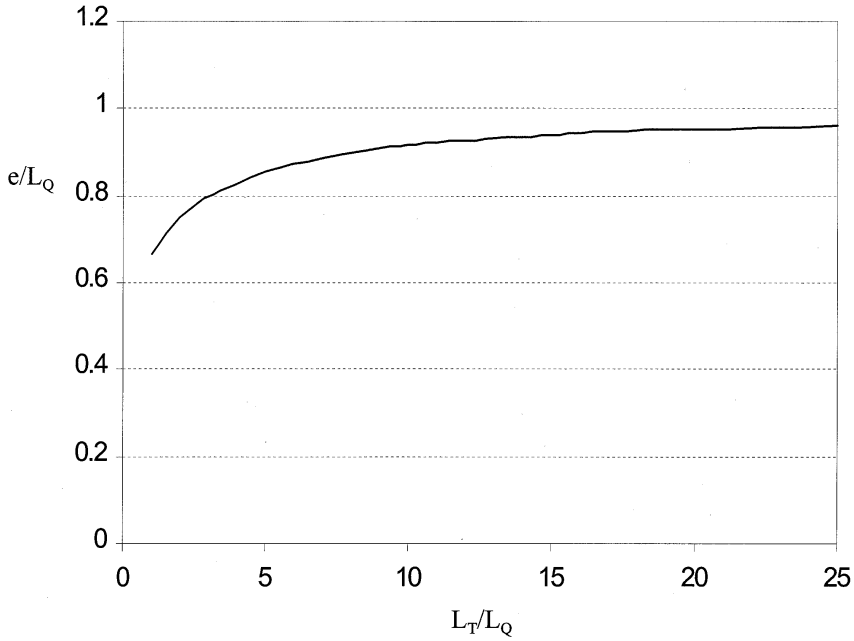

Figure 2. Eccentricity from the crack tip of Manu's singularity point.

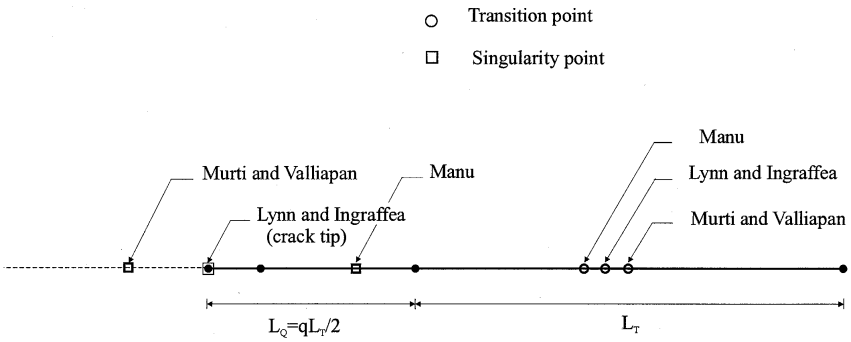

Figure 3. Comparison between the transition points and singularity points of three transition elements.

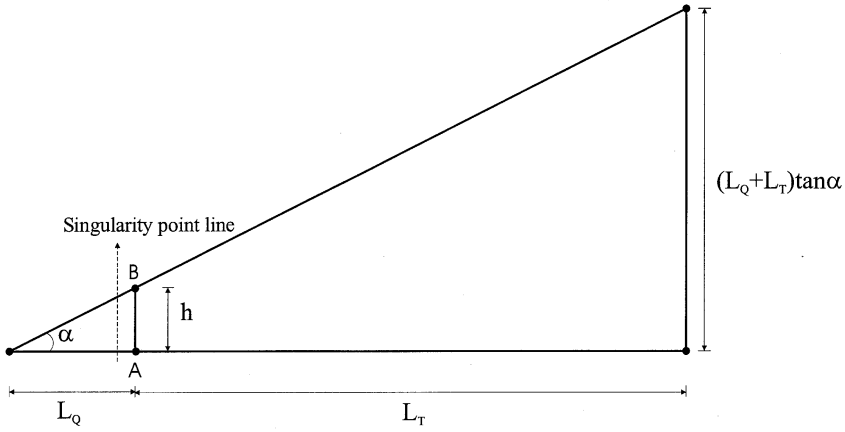

Figure 4. Singularity point line of a large TE (Manu).

singularity point line (the line that passes through the singularity points of the two edges) approaches AB. Also,

$$\frac{h}{(L_Q + L_T)\tan\alpha} = \frac{L_Q}{L_Q + L_T}. \tag{4}$$

Obviously, for large L_T/L_Q the ratio shown in (4) is very small. Therefore, for large L_T/L_Q, Manu's TE behaves approximately like an untied collapsed triangular QPE. Quarter-point elements are known to be more compliant than standard elements; therefore, if L_T/L_Q is large, the elements in the second row around the crack tip act as QPEs, and hence the stiffness of the system around the crack tip is reduced. This is the reason for Manu's numerical phenomenon. For large L_T/L_Q, using Manu's TEs, the SIF (calculated by displacement extrapolation method) will be grossly underestimated.

As was demonstrated by Lim et al. (1991), the original formulation of Lynn and Ingraffea is correct. Therefore, throughout this paper, when we write 'transition elements,' we refer to Lynn and Ingraffea's TEs. However, for comparison, in our numerical examples we use both Lynn and Ingraffea's and Manu's TEs.

3. Eight-noded transition elements

This section investigates the stress singularity within an eight-noded transition element, a problem that has been thoroughly studied for QPEs. Barsoum (1977) showed that, for a collapsed triangular QPE, stress is singular at the corner node for any ray emanating from the crack tip. He also indicated that, for an eight-noded quadrilateral QPE, stress is singular only along the two boundary lines. Hibbitt (1977) showed that the strain energy of these elements is unbounded. Later, Ying (1982) demonstrated that Hibbitt's proof was incorrect and that the strain energy of eight-noded quadrilateral elements is indeed bounded. Banks-Sills and Bortman (1984) showed that, for an eight-noded QPE, strain is singular in a small region adjacent to the crack tip, and the strain energy of this element is bounded. Later, Banks-Sills (1987) reconsidered this problem, and showed that these characteristics hold only for rectangular QPEs.

Using notation similar to that used by Hussain et al. (1981), we assume the length of the QPE to be unity. For a quadratic element, we know that

$$\begin{aligned} x &= \sum_{i=1}^{8} N_i(\xi, \eta) x_i, \\ y &= \sum_{i=1}^{8} N_i(\xi, \eta) y_i, \end{aligned} \tag{5}$$

where the x_i's and y_i's are nodal coordinates and the N_i's are shape functions. The eight-noded Serendipity element has the following shape functions in the normalized system

$$\begin{aligned} N_i &= [(1+\xi\xi_i)(1+\eta\eta_i) - (1-\xi^2)(1+\eta\eta_i) - (1-\eta^2)(1+\xi\xi_i)]\xi_i^2\eta_i^2/4 \\ &\quad +(1+\xi^2)(1+\eta\eta_i)(1-\xi_i^2)\eta_i^2/2 + (1-\eta^2)(1+\xi\xi_i)(1-\eta_i^2)\xi_i^2/2. \end{aligned} \tag{6}$$

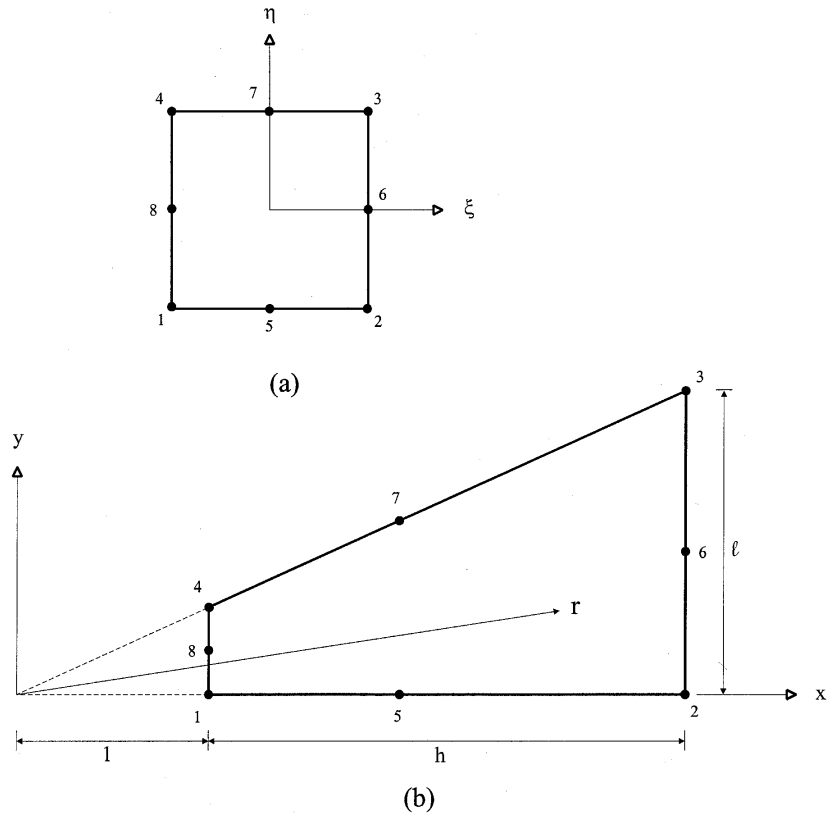

Figure 5. (a) Parent element in $\xi\eta$-plane, (b) Eight-noded transition element in the physical coordinate system.

Figure 5 shows an eight-noded element in physical and normalized coordinate systems. It can be shown that for this element we have[1]

$$x = \sqrt{1+h} + \tfrac{1}{2}h\xi + \tfrac{1}{2}[1 + \tfrac{1}{2}h - \sqrt{1+h}](1+\xi^2) = f(\xi),$$

$$y = \frac{\ell(1+\eta)}{2(1+h)}\{\sqrt{1+h} + \tfrac{1}{2}h\xi + \tfrac{1}{2}[1 + \tfrac{1}{2}h - \sqrt{1+h}](1+\xi^2)\} = \frac{\ell(1+\eta)}{2(1+h)} f(\xi). \quad (7)$$

Now let

$$K(h) = \tfrac{1}{2}[1 + \tfrac{1}{2}h - \sqrt{1+h}]. \quad (8)$$

It can be easily shown that

$$f(\xi) = K(h)\left(\xi + \frac{h}{4K(h)}\right)^2. \quad (9)$$

For this element

$$r = \sqrt{x^2 + y^2} = \frac{\sqrt{4(1+h)^2 + \ell^2(1+\eta)^2}}{2(1+h)} f(\xi). \quad (10)$$

[1] These symbolic computations were done by MATHCAD.

For $\eta =$ constant ($\theta =$ constant) we have

$$r = mf(\xi), \tag{11}$$

where m is a constant for any ray emanating from the crack tip. Therefore, from (9) and (11) we have

$$\xi + \frac{h}{4K(h)} = \frac{\sqrt{r}}{\sqrt{mK(h)}}. \tag{12}$$

The Jacobian of transformation is given by

$$[J] = \begin{bmatrix} \dfrac{\partial x}{\partial \xi} & \dfrac{\partial y}{\partial \xi} \\ \dfrac{\partial x}{\partial \eta} & \dfrac{\partial y}{\partial \eta} \end{bmatrix} = \begin{bmatrix} f'(\xi) & \dfrac{\ell(1+\eta)}{2(1+h)} f'(\xi) \\ 0 & \dfrac{\ell}{2(1+h)} f(\xi) \end{bmatrix} \tag{13}$$

and

$$\det[J] = \frac{\ell}{2(1+h)} f(\xi) f'(\xi). \tag{14}$$

Using Barsoum's (1977) notations

$$[J]^{-1} = \begin{bmatrix} \mathrm{I}_{11} & \mathrm{I}_{12} \\ \mathrm{I}_{21} & \mathrm{I}_{22} \end{bmatrix} = \begin{bmatrix} \dfrac{1}{f'(\xi)} & -\dfrac{1+\eta}{f(\xi)} \\ 0 & \dfrac{2(1+h)}{\ell f(\xi)} \end{bmatrix}. \tag{15}$$

For an eight-noded isoparametric element, displacements are expressed as

$$u = \sum_{i=1}^{8} N_i(\xi, \eta) u_i,$$

$$v = \sum_{i=1}^{8} N_i(\xi, \eta) v_i, \tag{16}$$

where u_i and v_i are nodal displacements. The derivatives of u, v with respect to ξ, η are, according to Barsoum (1977),

$$\frac{\partial u}{\partial \xi} = a_0 + a_1(1+\xi), \tag{17a}$$

$$\frac{\partial u}{\partial \eta} = b_0 + b_1(1+\xi) + b_2(1+\xi)^2, \tag{17b}$$

$$\frac{\partial v}{\partial \xi} = c_0 + c_1(1+\xi), \tag{17c}$$

$$\frac{\partial v}{\partial \eta} = d_0 + d_1(1+\xi) + d_2(1+\xi)^2, \tag{17d}$$

where a_0, a_1, b_0, b_1, b_2, c_0, c_1, d_0, d_1, and d_2 are constants for a given set of nodal displacements, and along any line $\theta =$ constant. We know that

$$\frac{\partial u}{\partial x} = \mathrm{I}_{11}\frac{\partial u}{\partial \xi} + \mathrm{I}_{12}\frac{\partial u}{\partial \eta}. \tag{18}$$

Substituting (15), (17a), and (17b) into (18) yields

$$\frac{\partial u}{\partial x} = \frac{a_0 + a_1(1+\xi)}{f'(\xi)} - \frac{b_0 + b_1(1+\xi) + b_2(1+\xi)^2}{f(\xi)}(1+\eta). \tag{19}$$

Equation (19) can be rewritten as

$$\begin{aligned}\frac{\partial u}{\partial x} &= \frac{\bar{a}_0 + \bar{a}_1\left(\xi + \dfrac{h}{4K(h)}\right)}{f'(\xi)} \\ &\quad - \frac{\bar{b}_0 + \bar{b}_1\left(\xi + \dfrac{h}{4K(h)}\right) + \bar{b}_2\left(\xi + \dfrac{h}{4K(h)}\right)^2}{f(\xi)}(1+\eta),\end{aligned} \tag{20}$$

where

$$\bar{a}_1 = a_1, \qquad \bar{a}_0 = a_0 + a_1\left(1 - \frac{h}{4K(h)}\right) \tag{21a}$$

$$\begin{aligned}\bar{b}_2 &= b_2, \qquad \bar{b}_1 = b_1 + 2b_2\left(1 - \frac{h}{4K(h)}\right), \\ \bar{b}_0 &= b_0 + b_1\left(1 - \frac{h}{4K(h)}\right) + b_2\left(1 - \frac{h}{4K(h)}\right)^2.\end{aligned} \tag{21b}$$

Substituting (12) into (20), we obtain

$$\begin{aligned}\frac{\partial u}{\partial x} &= \frac{\bar{a}_0 + \bar{a}_1\dfrac{\sqrt{r}}{\sqrt{mK(h)}}}{2\sqrt{\dfrac{K(h)}{m}}\sqrt{r}} - \frac{\bar{b}_0 + \bar{b}_1\dfrac{\sqrt{r}}{\sqrt{mK(h)}} + \bar{b}_2\dfrac{r}{mK(h)}}{\dfrac{r}{m}}(1+\eta) \\ &= A_0 + \frac{A_1}{\sqrt{r}} + \frac{A_2}{r}.\end{aligned} \tag{22}$$

Similarly, it can be shown that all the other displacement derivatives have the same form as (22). We cannot have any constraint on the nodal displacements; therefore, for any ray emanating from the crack tip, we have both $r^{-1/2}$ and r^{-1} strain singularities. Thus, for any ray emanating from the crack tip, ε_{xx}, ε_{yy} and ε_{xy} have both $r^{-1/2}$ and r^{-1} singularities.

Furgiuele and Luchi (1989) showed that for an untied collapsed triangular QPE (without any constraint on nodal displacements of the three nodes with the same position), ε_{rr} has $r^{-1/2}$ singularity while $\varepsilon_{\theta\theta}$ and $\varepsilon_{r\theta}$ retain both r^{-1} and $r^{-1/2}$ singularities. We show below that this is also the case for eight-noded TEs. We know that

$$\begin{aligned}\varepsilon_{rr} &= \frac{\partial u_r}{\partial r} = \frac{\partial u}{\partial x}\cos^2\theta + \frac{\partial v}{\partial y}\sin^2\theta + \left(\frac{\partial u}{\partial y} + \frac{\partial v}{\partial x}\right)\sin\theta\cos\theta \\ &= \left(\frac{\partial u}{\partial x}\cos\theta + \frac{\partial u}{\partial y}\sin\theta\right)\cos\theta + \left(\frac{\partial v}{\partial x}\cos\theta + \frac{\partial v}{\partial y}\sin\theta\right)\sin\theta. \end{aligned} \tag{23}$$

From (7) we have

$$\tan\theta = \frac{y}{x} = \frac{\ell(1+\eta)}{2(1+h)}. \tag{24}$$

We also know that

$$\begin{aligned}\frac{\partial u}{\partial x}\cos\theta + \frac{\partial u}{\partial y}\sin\theta &= \frac{\cos\theta}{f'(\xi)}\frac{\partial u}{\partial \xi} \\ &\quad + \frac{1}{f(\xi)}\left[-(1+\eta)\cos\theta + \frac{2(1+h)}{\ell}\sin\theta\right]\frac{\partial u}{\partial \eta}. \end{aligned} \tag{25}$$

The second term is responsible for the r^{-1} singularity. But from (24) it can be concluded that

$$-(1+\eta)\cos\theta + \frac{2(1+h)}{\ell}\sin\theta = 0. \tag{26}$$

Similarly,

$$\begin{aligned}\frac{\partial v}{\partial x}\cos\theta + \frac{\partial v}{\partial y}\sin\theta &= \frac{\cos\theta}{f'(\xi)}\frac{\partial v}{\partial \xi} \\ &\quad + \frac{1}{f(\xi)}\left[-(1+\eta)\cos\theta + \frac{2(1+h)}{\ell}\sin\theta\right]\frac{\partial v}{\partial \eta} \\ &= \frac{\cos\theta}{f'(\xi)}\frac{\partial v}{\partial \xi}. \end{aligned} \tag{27}$$

Therefore, ε_{rr} has only $r^{-1/2}$ singularity. The $\varepsilon_{r\theta}$ and $\varepsilon_{\theta\theta}$ have both $r^{-1/2}$ and r^{-1} singularities, characteristics similar to those of an untied collapsed triangular QPE. In summary, for eight-noded transition elements, ε_{xx}, ε_{yy}, ε_{xy}, $\varepsilon_{r\theta}$, and $\varepsilon_{\theta\theta}$ have both $r^{-1/2}$ and r^{-1} singularities and ε_{rr} has only $r^{-1/2}$ singularity.

Banthia (1985) studied collapsed eight-noded finite elements. He showed that, for collapsed triangular QPEs without any constraints on nodal displacements, whether or not the r^{-1} strain singularity can be modeled by the element depends strongly on the size of the element (and on the nodal displacements). He showed that, for small QPEs, r^{-1} dominates. Here, for a TE (and a constant QPE size), as L_T increases, the displacements of the nodes nonadjacent to the QPE increase, while the displacements of the three nodes adjacent to the QPE remain unchanged. Therefore, according to Banthia's argument, for this element $r^{-1/2}$ dominates, which is desirable in linear elastic fracture mechanics.

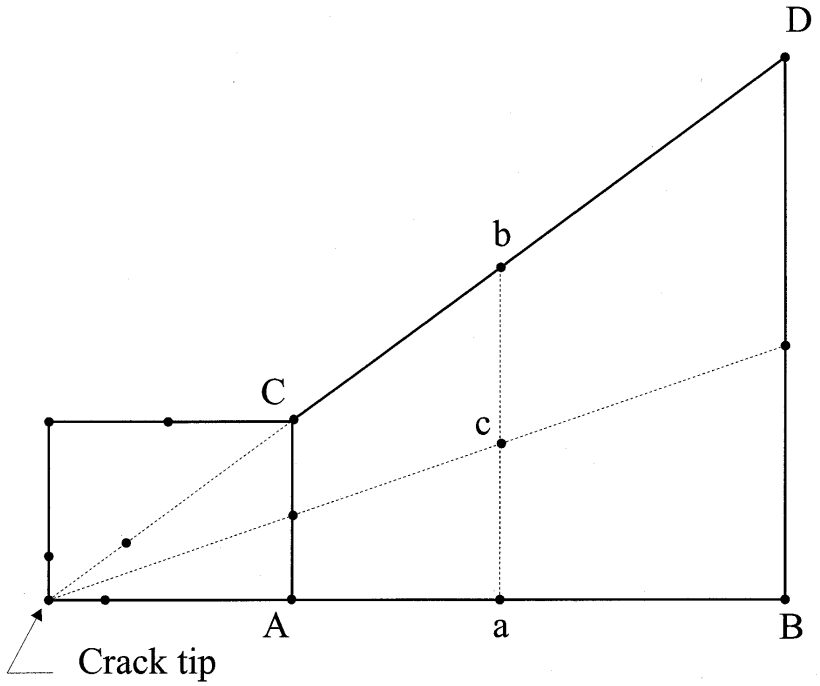

Figure 6. Assemblage of a nine-noded QPE and a nine-noded TE.

Up to now, no one has studied the effect of nine-noded transition elements on SIFs. In the next section, we formulate nine-noded transition elements and in Section 7, we perform numerical comparison of eight-noded and nine-noded TEs.

4. Nine-Noded Transition Elements

Banks-Sills and Einav (1987) studied nine-noded square quarter-point elements. They obtained two possible positions for the ninth node ($p = \frac{3}{8}, \frac{11}{32}$). They studied a square QPE and used square QPEs in their first numerical example, obtaining slightly better results than they achieved with eight-noded QPEs. Their second numerical example used nonrectangular quadrilateral nine-noded QPEs. In this case the results were less accurate than those obtained using eight-noded QPEs. Based on their numerical examples, Banks-Sills and Einav determined that nothing conclusive can be said about nine-noded QPEs. However, they did not notice that their formulation was based on the assumption that the element under study is square. In our numerical examples, the effects of TEs with nine-noded QPEs are studied.

Figure 6 shows an assemblage of a nine-noded TE and a nine-noded QPE. It can be easily shown that transition points for the edges AB and CD are the same as they are for an eight-noded TE. This is also the case for the ninth node; that is, the node '*c*' lies on the line segment ab. In Section 7, the effects of nine-noded TEs with different types of quarter-point elements are numerically studied.

The study of the strain singularity of nine-noded TEs can follow a pattern similar to that by which we studied eight-noded TEs. For a nine-noded TE, the transformation between physical and normalized systems can be shown to be the same as it is for an eight-noded TE. The

derivatives of u, v with respect to x, η are similar to eight-noded elements and can be expressed as

$$\frac{\partial u}{\partial \xi} = e_0 + e_1(1+\xi), \tag{28a}$$

$$\frac{\partial u}{\partial \eta} = f_0 + f_1(1+\xi) + f_2(1+\xi)^2, \tag{28b}$$

$$\frac{\partial v}{\partial \xi} = g_0 + g_1(1+\xi), \tag{28c}$$

$$\frac{\partial v}{\partial \eta} = h_0 + h_1(1+\xi) + h_2(1+\xi)^2, \tag{28d}$$

where e_0, e_1, f_0, f_1, f_2, g_0, g_1, h_0, h_1, and h_2 are constants for a given set of nodal displacements and along any line $\theta =$ constant ($\eta =$ constant).

Therefore, for nine-noded TEs, along any ray emanating from the crack tip, ε_{xx}, ε_{yy}, and ε_{xy} have both $r^{-1/2}$ and r^{-1} singularities. Also, ε_{rr} has only $r^{-1/2}$ singularity and $\varepsilon_{r\theta}$ and $\varepsilon_{\theta\theta}$ have both $r^{-1/2}$ and r^{-1} singularities. For large L_T, $r^{-1/2}$ singularity dominates.

Both eight-noded and nine-noded TEs are nonrectangular quadrilateral. In the next section, we study the potential of rectangular elements to model the strain singularity when they are used in the second row of finite elements around the crack tip.

5. Semi-transition elements

Transition elements are nonrectangular quadrilateral elements that are used in the second layer around the crack tip and whose two edges are along the crack tip. Assume that we want to use a mesh whose elements are only rectangular; therefore the elements in the second layer from the crack tip are also rectangular. Around the crack tip are four rectangular QPEs, as shown in Figure 7. In the second layer are twelve elements. Any of the eight shaded elements has one edge along the crack tip; the parallel edge is not along the crack tip. If we put the mid-node of the edge along the crack tip at the transition point, this rectangular element is called, semi-transition element (STE).

Nothing can be said about semi-transition elements before a numerical analysis is performed. But we can guess that they cannot be as effective as TEs, because: (1) they cannot have large L_T/L_Q ratio because in that case we will have an element with a large aspect ratio, and (2) these elements have only one singular ray. We investigate numerically the effects of these elements on SIFs in Section 7.

6. Layered transition elements

In a finite element mesh, around the crack tip we can have only one layer of crack-tip elements, because crack-tip elements have to have one edge in common with a crack face. However, we do not have such a restriction for TEs. Murti and Valliapan (1986) introduced the concept of layered transition elements (LTE). Their idea, while worthy, was unfortunately presented using an incorrect formulation. We present below the correct formulation of layered transition elements.

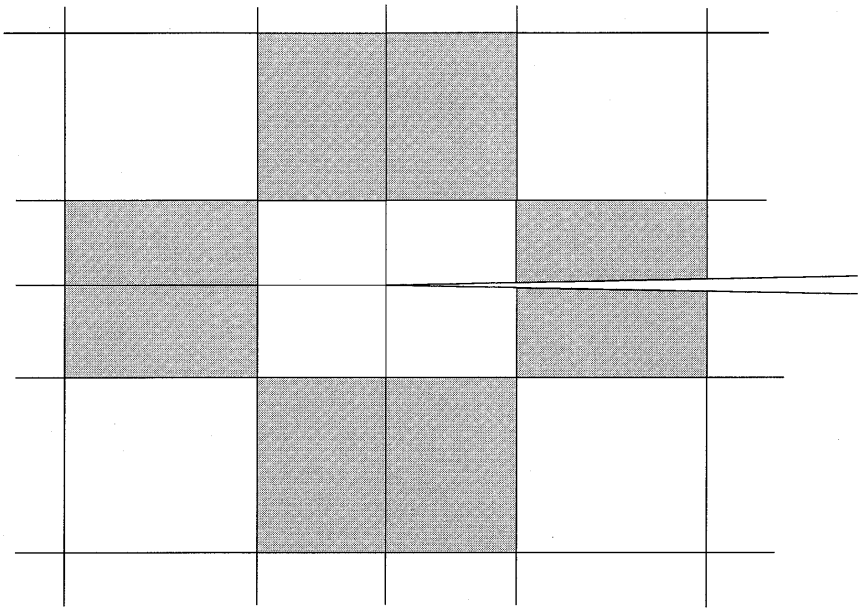

Figure 7. A rectangular mesh around the crack tip; dashed elements are semi-transition elements.

Murti and Valliapan's Figure 7 shows the assemblage of three transition elements and a quarter-point element. For all the TEs, the singularity point lies at the crack tip. The length of the nth TE is denoted by L_{Tn}. For finding the nth transition point it is assumed that the QPE and the $n-1$ other TEs before the nth TE constitute a fictitious QPE whose length is denoted by L'_Q. Thus,

$$L'_{Qn} = L_Q + \sum_{i=1}^{n-1} L_{Ti}, \tag{29a}$$

$$q_n = \frac{2L_Q}{L_T} = \frac{2L_Q + 2\sum_{i=1}^{n-1} L_{Ti}}{L_{Tn}}, \tag{29b}$$

Therefore, for each TE we have a q_n. Substituting q_n from (29) into (1) we obtain

$$\tfrac{1}{2}p_n = \frac{1 - q_n + \sqrt{q_n^2 + 2q_n}}{2}. \tag{30}$$

Layered transition elements are useful in problems where both L_Q/a and L_T/L_Q (of the first layer of TEs) are small. The effects of the LTEs are shown numerically in Section 7.

7. Numerical examples

Up to now, all investigations of the effects of TEs have considered only TEs with collapsed triangular QPEs. In this study collapsed triangular, eight-noded, and nine-noded quadrilateral

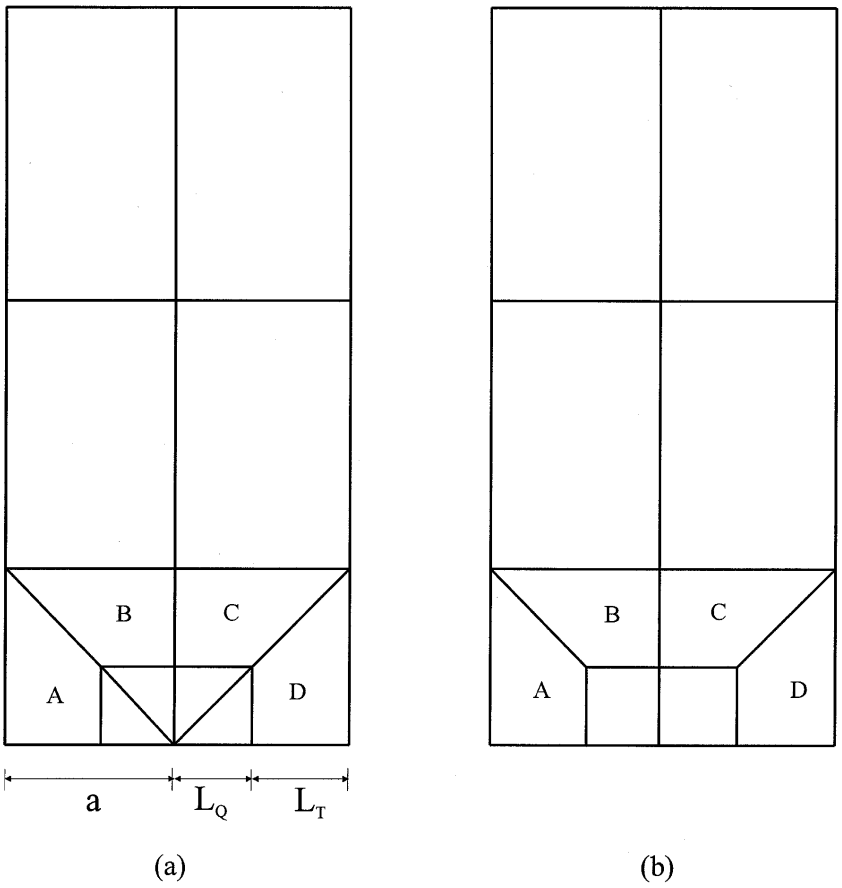

Figure 8. A quarter of a double-edge-cracked plate; elements A, B, C, and D are transition elements. (a) with triangular QPEs; (b) with rectangular QPEs.

QPEs are considered. In all the numerical analyses presented here, a displacement extrapolation method with linear regression is used and a plane stress condition is assumed. For the displacement extrapolation method, the normal displacement component (v) along the crack face is used. In all these numerical examples the material used is steel with $E = 30000$ ksi and $\nu = 0.3$. Four geometries are considered for the numerical analyses:

(1) Double-edge-cracked plate under uniform remote stress.
(2) Arch-shaped specimen in bending.
(3) Three-point bend specimen.
(4) Center-cracked plate under uniform remote stress.

In the first two numerical examples we compare all possible combinations of TEs and QPEs, in order to identify the combination that yields the most accurate SIFs.

As the first numerical example, a double-edge-cracked plate under uniform remote stress is considered (Figure 8). The dimensions are the same as those of Lynn and Ingraffea's and Manu's numerical examples. Our mesh is similar to that of Lynn and Ingraffea. Eight different cases are examined (in each case both Lynn and Ingraffea's and Manu's TEs were used for comparison):

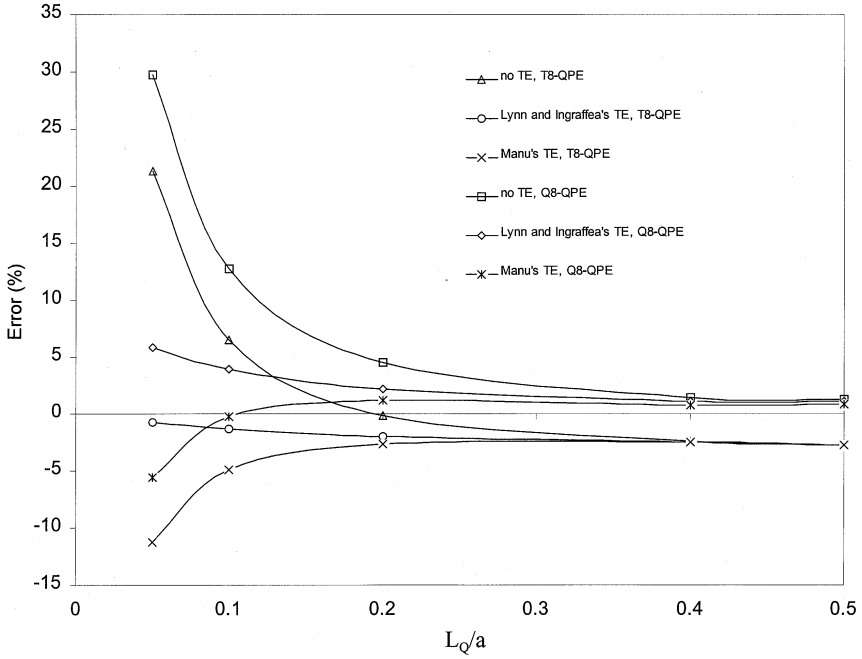

Figure 9. Percentage error of the calculated K_{I} values with collapsed triangular (T8) and rectangular (Q8) QPEs.

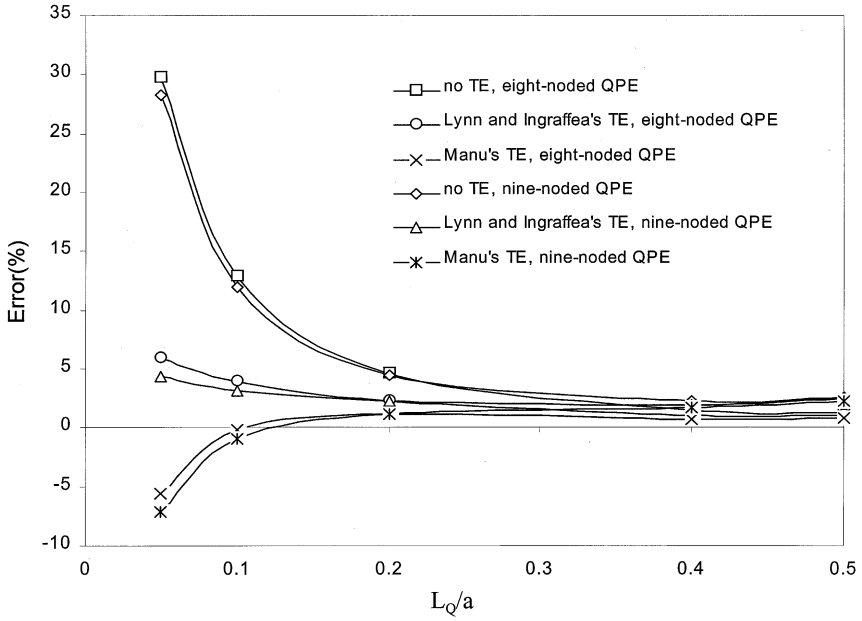

Figure 10. Comparison between the effects of TEs with eight-noded and nine-noded ($p = 11/32$) QPEs.

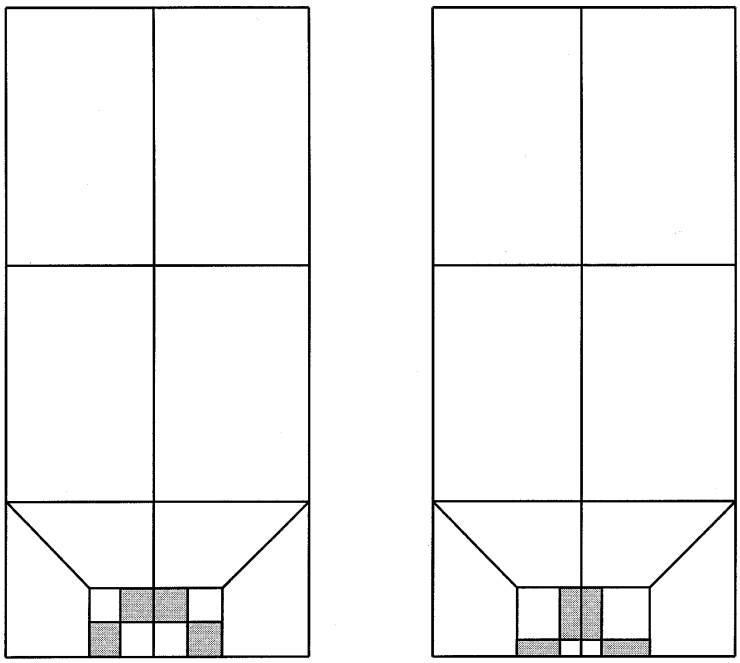

Figure 11. A quarter of a double-edge-cracked plate; shaded elements are semi-transition elements. (a) $L_T/L_Q = 1$; (b) $L_T/L_Q = 2$.

(1) Collapsed triangular QPEs with eight-noded TEs.
(2) Collapsed triangular QPEs with nine-noded TEs.
(3) Eight-noded QPEs with eight-noded TEs.
(4) Eight-noded QPEs with nine-noded TEs.
(5) Nine-noded QPEs ($p = \frac{3}{8}$) with eight-noded TEs.
(6) Nine-noded QPEs ($p = \frac{3}{8}$) with nine-noded TEs.
(7) Nine-noded QPEs ($p = \frac{11}{32}$) with eight-noded TEs.
(8) Nine-noded QPEs ($p = \frac{11}{32}$) with nine-noded TEs.

In this example, the eight-noded and nine-noded QPEs are square. Figure 9 shows the percentage error that occures when collapsed triangular and eight-noded square QPEs are used, versus L_Q/a. The curves are similar to those of Lynn and Ingraffea. As can be seen for small L_Q/a, using TEs improves the accuracy of the SIFs. But L_Q/a is not the only important factor. Lynn and Ingraffea did not explore the fact that, by using this specific mesh, when reducing L_Q/a, the L_T/L_Q automatically increases; actually $L_T/L_Q = (L_Q/a)^{-1} - 1$. Using this mesh we can change these two parameters simultaneously and see the effects of the TEs more easily.

If we have small L_Q/a and small L_T/L_Q, the TEs will have no important effect because in that case the (standard) elements in the third layer should be able to model a part of the singularity. But they cannot, and this is a source of error.

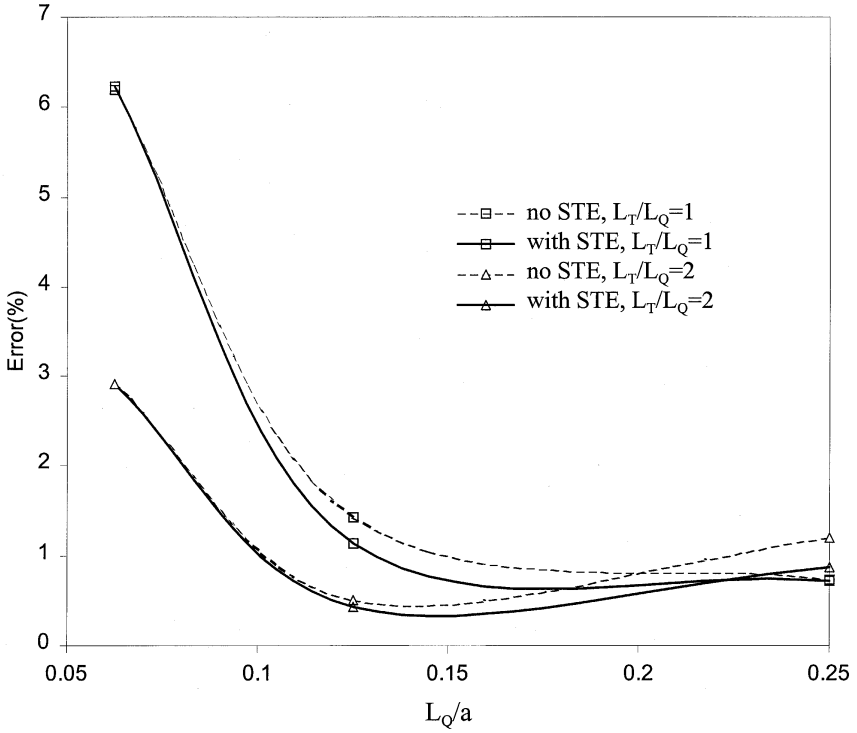

Figure 12. Percentage error of the calculated K_I values with STEs and with eight-noded QPEs.

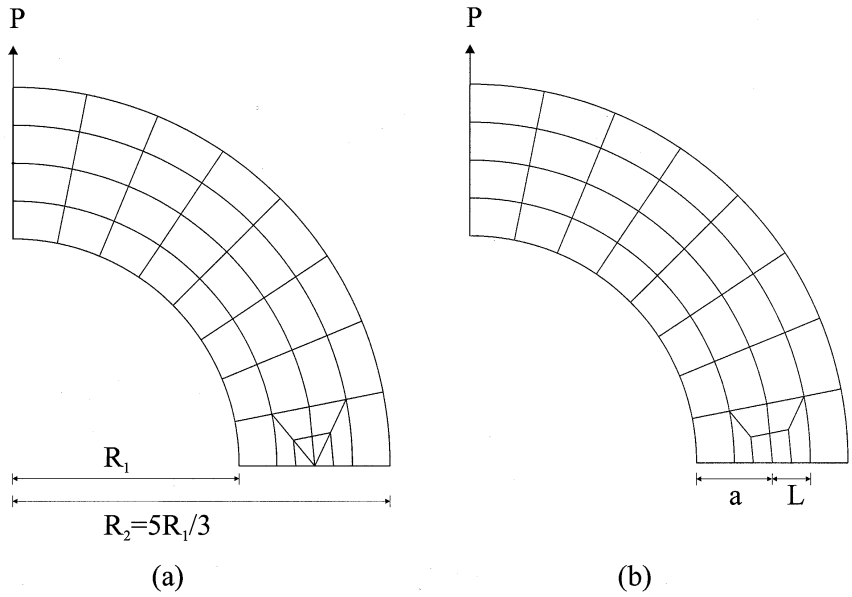

Figure 13. One half of an arch-shaped specimen in bending. (a) collapsed triangular QPEs; (b) quadrilateral QPEs.

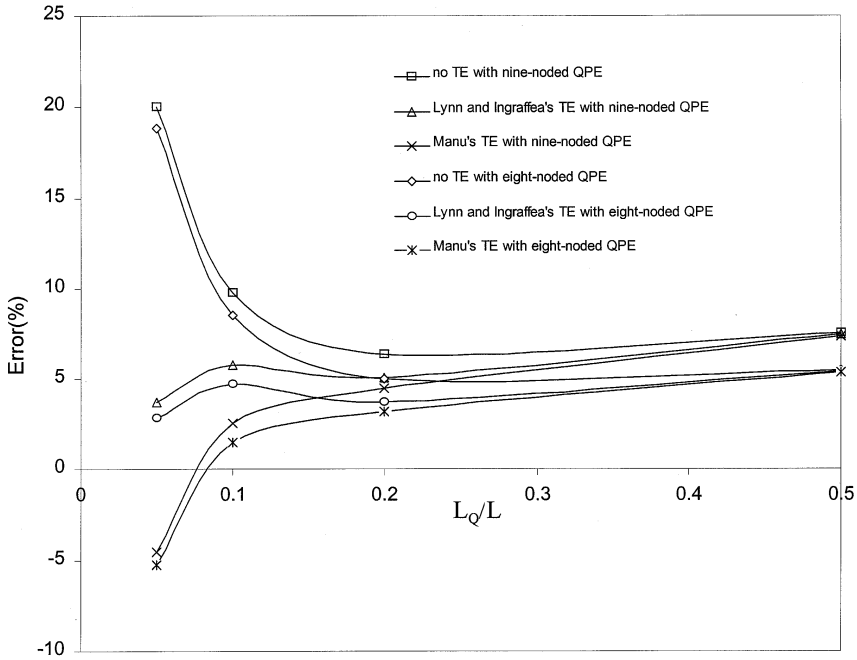

Figure 14. Comparison of eight-noded and nine-noded nonrectangular quadrilateral QPEs for an arch-shaped specimen in bending.

With collapsed triangular and rectangular eight-noded QPEs, eight-noded and nine-noded TEs have exactly the same effects on the accuracy. So the TE in Figure 9 stands for both eight-noded and nine-noded TEs. Qualitatively, TEs have similar effects with either QPE. Then nine-noded QPEs ($p = \frac{3}{8}$) are used. They behave exactly the same as eight-noded QPEs in this case and the effects of the eight-noded and nine-noded TEs are also exactly the same for this QPE. Figure 10 compares the effects of TEs with eight-noded and with nine-noded ($p = \frac{11}{32}$) QPEs. As can be seen, the qualitative effect of the TEs with nine-noded QPEs ($p = \frac{11}{32}$) is similar to that of the other cases. In this case nine-noded QPEs give slightly better results. Again, eight-noded and nine-noded TEs have exactly the same effects.

Figure 11 shows two other meshes for the double-cracked plate. In these meshes only rectangular elements are used for studying semi-transition elements. In case (a), $L_T/L_Q = 1$, and in case (b), $L_T/L_Q = 2$. In Figure 12, the effects of the STEs are shown for $L_T/L_Q = 1, 2$. As can be seen, the STEs have a marginal effect; they improve the accuracy a little. For both cases, when the mid-node of the parallel edge is placed at the transition point the results are a little worse than they are in the case without STEs. Therefore, for creating STEs, only the position of the mid-node of the edge that is along the crack tip must be changed. STEs have two problems (as is pointed out in Section 5). The first problem is that they have only one singular ray; the second problem is that for STEs we cannot have large L_T/L_Q because then we have an element with a very large aspect ratio, which is not acceptable in finite element analysis. In all the cases for large L_T/L_Q (and small L_Q/a), Manu's TEs give very inaccurate results, as we explained in Section 2.

As the second numerical example, an arch-shaped specimen in bending is considered. Only one half of the specimen is modeled as shown in Figure 13. The inner and outer radii of the specimen are R_1 and $R_2(= 5R_1/3)$, respectively, and $a = R_1/3$. In this case nonrectangular

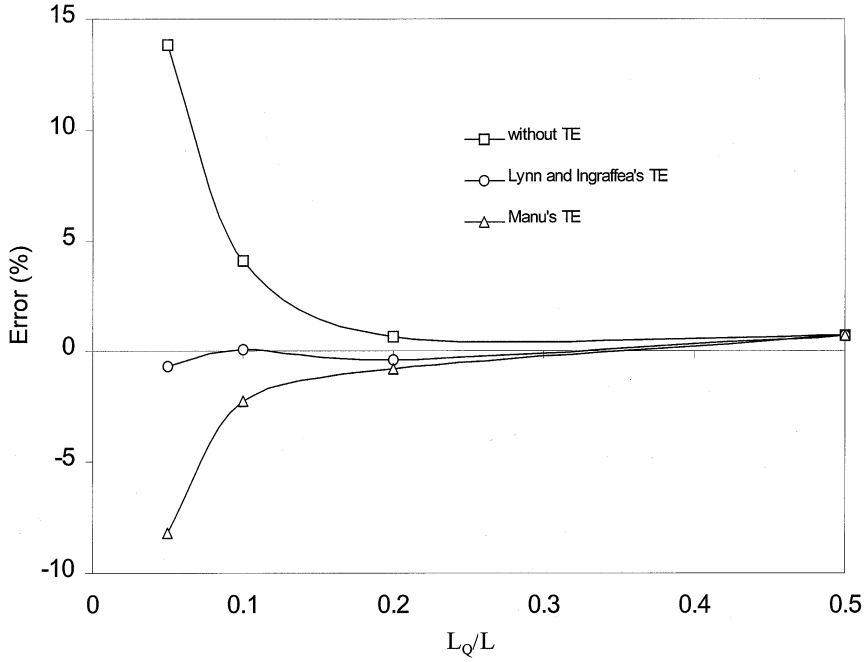

Figure 15. Percentage error of the calculated K_{I} values for an arch-shaped specimen using collapsed triangular QPEs.

quadrilateral QPEs are used. Here $L_Q + L_T = L$ is assumed to be constant ($L = a/2$). As was done for the first numerical example, eight cases are investigated. In Figure 14, eight-noded and nine-noded ($p = \frac{11}{32}$) QPEs and the effects of the TEs are compared. Clearly, eight-noded QPEs give better results. Eight-noded TEs have almost the same effect as nine-noded TEs; actually, the difference between them is very small.

In Figure 15, the effect of TEs with collapsed triangular QPEs is shown. The effects of eight-noded and nine-noded TEs are almost the same. In Figure 16, nine-noded QPEs ($p = \frac{3}{8}$, $p = \frac{11}{32}$) with and without TEs are compared. As can be seen, without TEs both nine-noded QPEs behave almost the same, but when using TEs, $p = \frac{11}{32}$ gives slightly better results. Again with nine-noded QPEs ($p = \frac{3}{8}$, $p = \frac{11}{32}$), eight-noded and nine-noded TEs have almost the same effects. Again Manu's TEs badly underestimate K_{I} for large L_T/L_Q.

In the third and fourth numerical examples, the effect of layered TEs is studied. In both cases, two layered TEs are considered. The third numerical example examines a three-point bend specimen (Figure 17). Here, $L = L_Q + L_{T1} + L_{T2} (L = a/4)$ is assumed to be constant and $L_{T1}/L_Q = 2$. We consider three cases: one without using TEs, one using only one layer of TEs, and one using two layers of TEs. The first layer of TEs has a small $L_T/L_Q (= 2)$. So, as can be seen in Figure 18, these TEs have almost no effect. When L_Q/a is small, using two layers of TEs improves the accuracy of the results.

In the fourth numerical example the same three part investigation is conducted for a center-cracked plate under uniform remote stress (Figure 19). The meshes are the same for the two numerical examples; for the three-point bend specimen one-half of the beam, and for the center-cracked plate a quarter of the plate are modeled. As can be seen in Figure 20, the results are similar to those depicted in Figure 18.

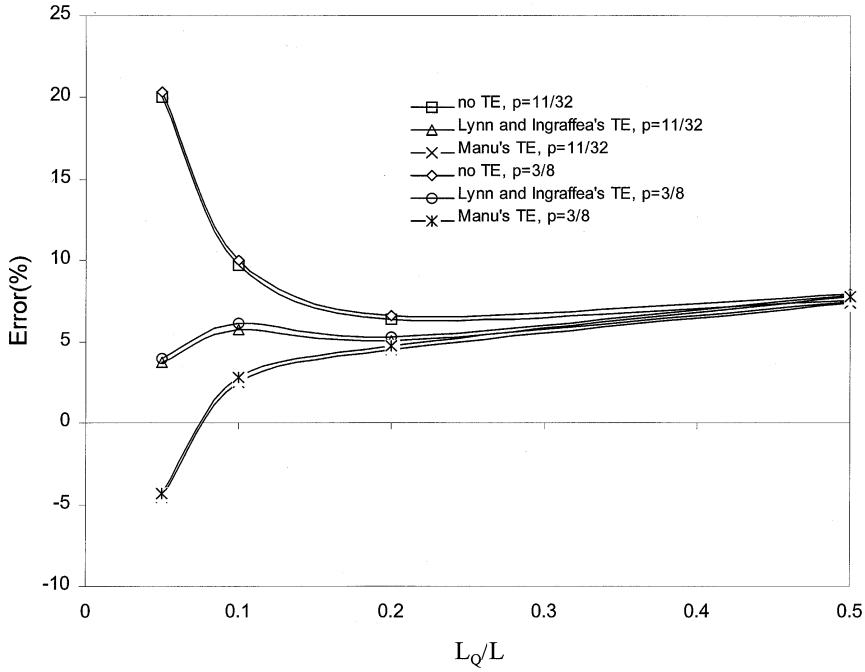

Figure 16. Comparison between nine-noded QPEs with $p = 11/32$ and $p = 3/8$ for an arch-shaped specimen in bending.

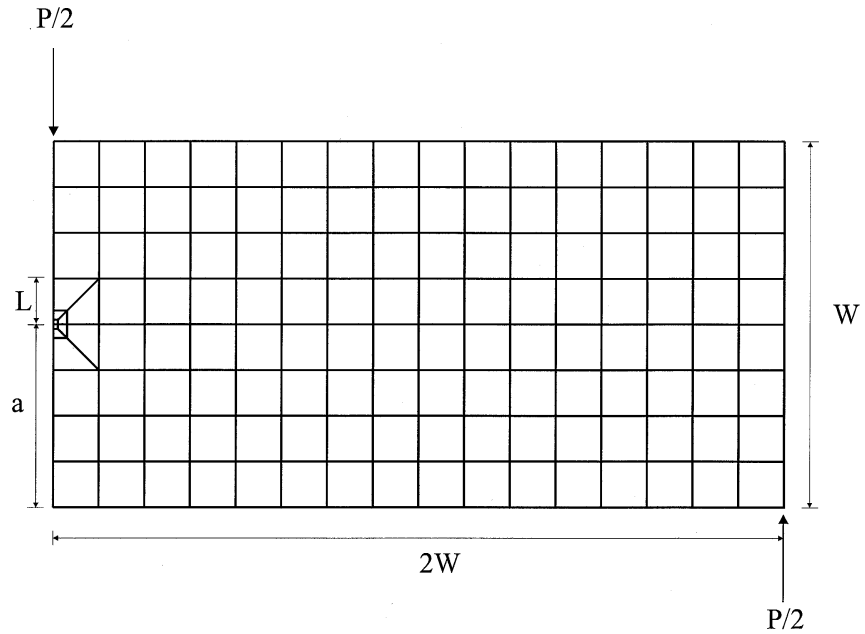

Figure 17. One half of a three-point bend specimen.

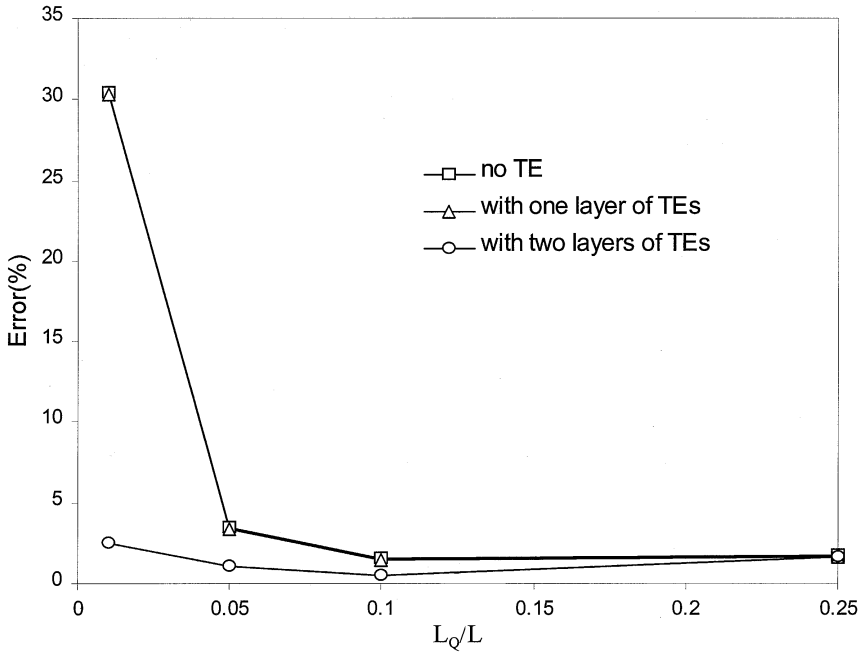

Figure 18. Effect of layered TEs for a three-point bend specimen, $L_{T1}/L_Q = 2(L = L_Q + L_{T1} + L_{T2})$.

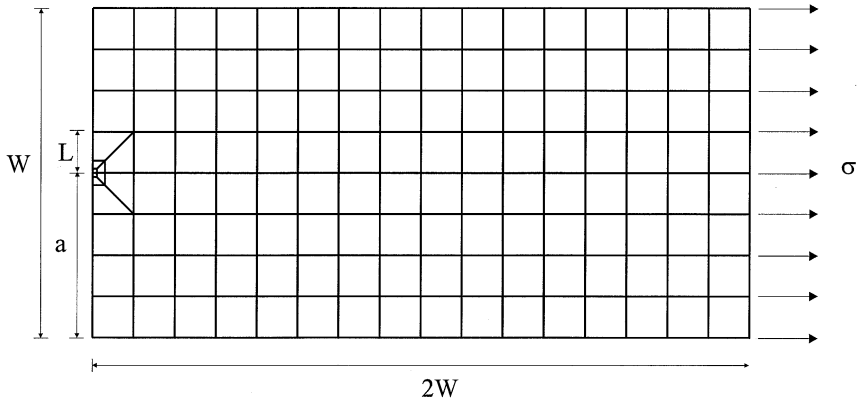

Figure 19. A quarter of a center-cracked plate under uniform remote stress.

8. Conclusions

In this paper, a detailed comparison of Lynn and Ingraffea's and Manu's TEs was offered. We showed that large Manu's TEs reduce the stiffness of the system around the crack tip and hence grossly underestimate SIFs. Strain singularity of eight-noded TEs was investigated. For these TEs along any ray emanating from the crack tip, ε_{xx}, ε_{yy}, ε_{xy}, $\varepsilon_{r\theta}$, and $\varepsilon_{\theta\theta}$ have both r $^{-1/2}$ and r $^{-1}$ singularities, while ε_{rr} has only $r^{-1/2}$ singularity. But for large L_T, $r^{-1/2}$ dominates for all strains. Nine-noded TEs were formulated whose transition points were shown to be the same as those for eight-noded TEs. The strain singularity is also the same for both nine-noded and eight-noded TEs. We showed numerically that transition elements have qualitatively the same effect, whether they are used with collapsed triangular QPE, eight-noded rectangular and nonrectangular quadrilateral QPEs, or nine-noded rectangular and nonrectangular quadri-

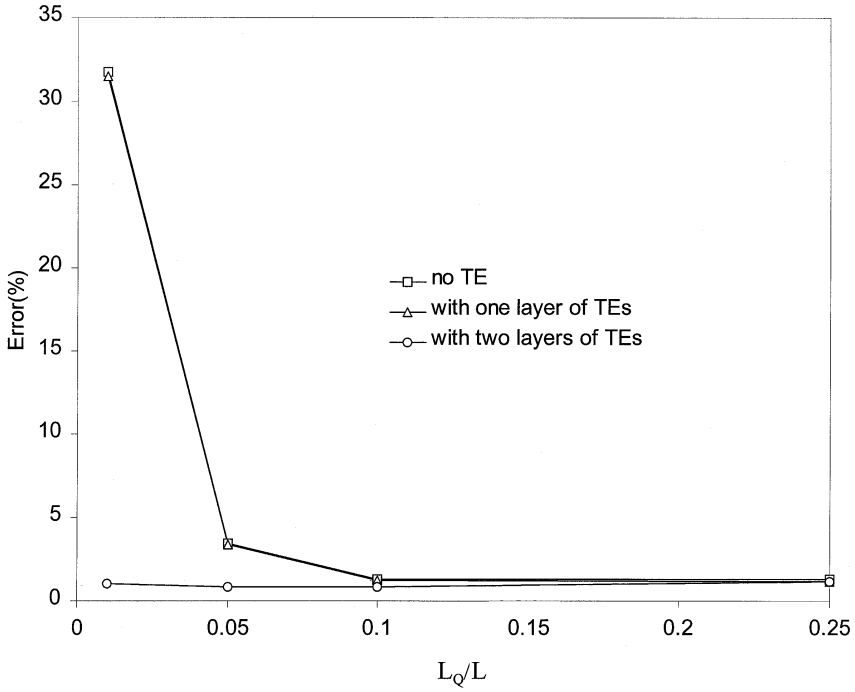

Figure 20. Effect of layered TEs for a center-cracked plate under remote uniform stress, $L_{T1}/L_Q = 2(L = L_Q + L_{T1} + L_{T2})$.

lateral QPEs ($p = \frac{3}{8}, \frac{11}{32}$). Also eight-noded and nine-noded TEs have almost the same effect; so eight-noded TEs are preferable because they have fewer degrees of freedom.

Semi-transition elements were defined and it was shown that they have a marginal effect on SIFs. The correct formulation of layered transition elements was presented and it was observed that when, for the first layer of TEs, L_T/L_Q is small, using the second layer of TEs can improve the accuracy of the calculated SIFs.

Incorporating a layer of TEs into a finite element mesh produces results that always are better than or equal to those obtained when TEs are not used. Generally, around the crack tip and at a certain distance from it, strain singularity dominates (this is called the singularity radius). Inside the strain singularity region, finite elements should be able to model the singularity to obtain the best results with the same mesh. If crack-tip elements are large (that is, if L_Q is equal to or greater than the singularity radius), using TEs has no improving effect. When L_Q is small, TEs can improve the accuracy. If L_T/L_Q is large, then $L_Q + L_T$ is equal to or greater than the singularity radius. In this case using a layer of TEs improves the calculated SIFs. If L_T/L_Q is small, the first layer of TEs has a marginal effect and a second layer of TEs can improve the accuracy, and so on. The main advantage of using TEs is that with them the calculated SIFs are less dependent on L_Q/a than without them.

In summary, transition elements can be practically useful if layered transition elements are used in the singularity region around the crack tip. Since the size of the singularity region is problem dependent we can assume that the radius of this region is 20–30 percent of the characteristic length of the crack (a).

Appendix 1

By comparing Figure 1 of (Lynn and Ingraffea, 1978) and Figure 1 of (Hussain, et al., 1981) it can be shown that

$$h = \frac{L-1}{2}, \qquad q = \frac{2}{L-1}, \qquad p = \frac{2(\beta L - 1)}{L-1}. \tag{31}$$

Substituting (31) into (5) of (Lynn and Ingraffea, 1978) we end up at (6) of (Hussain, et al., 1981). Therefore, Lynn and Inraffea's transition element is the same as that of Hussain, et al.

References

Banks-Sills, L. and Bortman, Y. (1984). Reappraisal of the quarter-point quadrilateral element in linear elastic fracture mechanics'. *International Journal of Fracture* **25**, 169–180.

Banks-Sills, L. (1987). Quarter-point singular elements revised, *International Journal of Fracture* **34**, R63–R69.

Banks-Sills, L. and Einav, O. (1987). On singular, nine-noded, distorted, isoparametric elements in linear elastic fracture mechanics. *Computers and Structures* **25**, 445–449.

Banthia, V. (1985). Singularity of collapsed Q-8 finite element. *International Journal for Numerical Methods in Engineering* **21**, 959–965.

Barsoum, R. S. (1976). On the use of isoparametric finite elements in linear fracture mechanics. *International Journal for Numerical Methods in Engineering* **10**, 25–37.

Barsoum, R. S. (1977). Triangular quarter-point elements as elastic and perfectly-plastic crack-tip elements. *International Journal for Numerical Methods in Engineering* **11**, 85–98.

Furgiuele, F. M. and Luchi, M. L. (1989). A note on some crack tip elements employed in two-dimensional elasto-plastic fracture mechanics. *Engineering Fracture Mechanics* **33**, 831–837.

Henshell, R. D. and Shaw, K. G. (1975). Crack tip finite elements are unnecessary. *International Journal for Numerical Methods in Engineering* **9**, 495–507.

Hibbitt, H. D. (1977). Some properties of isoparametric elements. *International Journal for Numerical Methods in Engineering* **11**, 1980–83.

Horva'th, A. (1994). General forming of transition elements. *Communications in Numerical Methods in Engineering* **10**, 267–273.

Hussain, M. A., Vasilakis, J. D., and Pu, S. L. (1981). Quadratic and cubic transition elements. *International Journal for Numerical Methods in Engineering* **17**, 1397–1406.

Lim, I. L., Johnston, I. W., and Choi, S. K. (1991). The use of transition elements. *Engineering Fracture Mechanics* **40**, 975–983.

Lynn, P. P. and Ingraffea, A. R. (1978). Transition elements to be used with quarter-point crack- tip elements. *International Journal for Numerical Methods in Engineering* **12**, 1031–1036.

Manu, C. (1986). Quadratic isoparametric elements as transition elements. *Engineering Fracture Mechanics* **24**, 509–512.

Murti, V. and Valliapan, S. (1986). A universal optimum quarter-point element. *Engineering Fracture Mechanics* **25**, 237–258.

Ying, L-A (1982). A note on the singularity and strain energy of singular elements. *International Journal for Numerical Methods in Engineering* **18**, 31–39.